ULTRAVIOLET OUTBURST IN THE M87 JET: SUBLUMINAL OR SUPERLUMINAL?

Giorgio Capezzali[a]

Abstract: The observations of the M87 jet with the STIS instrument mounted on board the Hubble Space Telescope revealed that an outburst originating in the HST-1 knot occurred. Measuring the dimensions of the outburst in the epochs between 2001 July 30 and 2003 July 27 and correcting for optical illusion an expansion velocity $v/c = 0.99893 \pm 0.00007$ is found. However, the relativistic model fails to correctly predict the dimensions of the source and the outburst brightness. For this reason, as the apparent motion suggests, a superluminal mechanical model where even the light rays travel faster than light is introduced. By applying this model to correct for optical illusion an expansion velocity $v/c = 21.8 \pm 0.7$ is found along with reasonable source dimensions and brightness. This result, the study of the apparent motion of features in the M87 jet and the time-of-flight measurements of muonic neutrinos seem to confirm the possibility to travel faster than light. That does not imply a refusal of special relativity. Instead only the common interpretations of it are refused. Without them, we will also see that the so-called twin paradox does not have any reason to exist.

1. INTRODUCTION

The galaxy M87 when seen through a telescope appears as a giant elliptical galaxy consisting of a central part looking like a normal elliptical surrounded by an extended fainter halo of stars. When seen at short exposures instead, the galaxy M87 appears as a normal E_0 galaxy with a blue jet coming out of its nucleus (see figure 18.15 in ref. [1]).

M87 nucleus is classified as an active galactic nucleus (AGN) since it has been observed to be subject to violent activity. The emitted radiation cannot be produced by stars, and the most plausible source of energy in this AGN is then thought to be the gravitational energy generated by a supermassive black hole (mass $> 10^8$ $M_\odot$). A beam carrying energy and charged particles generates from the accretion disk around the supermassive black hole. The kiloparsec-scale jet coming out of the AGN of M87 galaxy has been observed at radio, optical, UV, and X-ray wavelengths. These high-resolution observations revealed distinct regions along the jet of enhanced emission or knots.

As illustrated in ref. [2], the HST-1 knot located $0.85''$ from the nucleus of M87 galaxy was an inconspicuous region of enhanced emission until 2000 February when its intensity began to increase over its quiescent level.

Between 2001 and 2008 the flaring activity was detected in radio, optical and X-rays. Very high energy γ-ray emission ($E > 100$ GeV) also occurred. Two episodes of enhanced VHE activity have been detected in 2005 and 2008. The multi-wavelength light curve of M87 from 2001 to 2011 can be found in ref. [3] where the separate fluxes for the core and HST-1 are shown.

[a] giorgio.capezzali@gmail.com

In this article we will focus our attention on the observations in the near-ultraviolet (NUV) obtained with the Space Telescope Imaging Spectrograph (STIS). The first image of the series was taken in 1999 May 17 when the HST-1 was an unremarkable knot along the jet, while the last image was taken in 2003 July 27 when the outburst had already occurred. Images of the knot at later dates are not available because the STIS stopped functioning in 2004 August due to an electronic failure. Further observations of the M87 jet taken with other instruments at different wavelengths will not be considered here.

2. SUBLUMINAL OUTBURST

2.1 RELATIVISTIC CORRECTION FOR OPTICAL ILLUSION

We consider bright relativistic matter travelling at constant speed v and forming an angle θ with respect to the direction OT as illustrated in Figure 1.
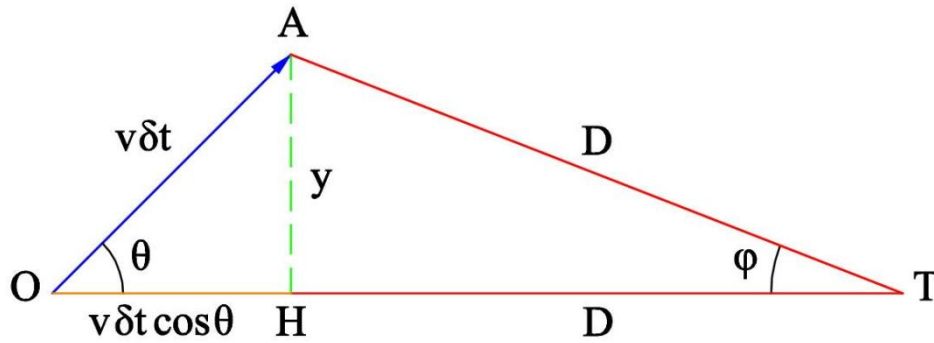
Figure 1 – *Distance travelled by two light rays emitted from bright matter with time separation δt.*

At time t_1 a light ray leaves the bright matter from point O, while at time t_2 a second light ray leaves the bright matter from point A. We define the temporal separation between the two emission times as $\delta t = t_2 - t_1$. Since OT = OH + HT, the first light ray reaches the observer in T at time:

$$t_{1a} = t_1 + \frac{D + v\delta t\cos\theta}{c}$$

where D is the length of HT and c the speed of light in vacuum.
We suppose that the separation of T from O is such that φ is small enough to have the two distances AT and HT equal, AT= HT = D. Hence, the second light ray reaches the observer in T at time:

$$t_{2a} = t_2 + \frac{D}{c}$$

In consequence, the observer in T will see the two light rays separated by an apparent interval of time:

$$\delta t_a = t_{2a} - t_{1a} = t_2 - t_1 - \frac{v\delta t\cos\theta}{c} = \delta t\left(1 - \frac{v}{c}\cos\theta\right)$$

It follows that the relation between the true interval of time δt separating the two emission processes and the observed one δt_a is given by:

$$\delta t = \frac{\delta t_a}{1 - \frac{v}{c}\cos\theta} \tag{1}$$

Now the projection y on the sky plane of the distance travelled by the bright matter in the real interval of time δt is (see Figure 1):

$$y = v\delta t\sin\theta = \frac{v\delta t_a \sin\theta}{1 - \frac{v}{c}\cos\theta}$$

This quantity has its maximum for an angle θ such that $dy/d\theta = 0$. The derivative of y with respect to θ is calculated as follows:

$$\frac{dy}{d\theta} = \frac{v\delta t_a \cos\theta}{1 - \frac{v}{c}\cos\theta} - \frac{v\delta t_a \sin\theta}{\left(1 - \frac{v}{c}\cos\theta\right)^2}\frac{v}{c}\sin\theta =$$

$$= \frac{1}{\left(1 - \frac{v}{c}\cos\theta\right)^2}v\delta t_a\left(\cos\theta - \frac{v}{c}\cos^2\theta - \frac{v}{c}\sin^2\theta\right) =$$

$$= \frac{v\delta t_a}{\left(1 - \frac{v}{c}\cos\theta\right)^2}\left(\cos\theta - \frac{v}{c}\right)$$

So, it will be $dy/d\theta = 0$ when $\cos\theta = v/c$ or $\theta = \arccos(v/c)$. Since at this angle $\sin\theta = (1 - v^2/c^2)^{1/2}$, the maximum projection y_s on the sky plane of the distance travelled by the bright matter in the observed interval of time δt_a is:

$$y_s = \frac{v\delta t_a\sqrt{1 - \frac{v^2}{c^2}}}{1 - \frac{v^2}{c^2}} = \frac{v\delta t_a}{\sqrt{1 - \frac{v^2}{c^2}}} \tag{2}$$

The relations derived in this section will be useful in the next one to correct for optical illusion all the measurements derived from the STIS images.

2.2 SUBLUMINAL EXPANSION VELOCITY OF THE OUTBURST

The calibrated flat-fielded science files (flt) used for the study of the HST-1 outburst were obtained from the Mikulski Archive for Space Telescopes (MAST)[b].
These files are the images at different epochs of the M87 jet carried out using the NUV/MAMA detector and the F25QTZ filter. The photometry of the calibrated files features a pivot wavelength and an RMS bandwidth varying with the image considered. However, the exact values are found in the intervals 2360÷2362 Å and 421÷422 Å respectively. Instead the F25QTZ filter has its maximum throughput wavelength at 2364.8 Å and a width of 995.1 Å.


All the files were viewed by using the software *fv 5.3* provided by GSFC/NASA. The same software *fv 5.3* was also used to take measurements on the various images at different epochs.

Figure 2 shows the M87 jet and a zoom of the HST-1 knot in 1999 May 17. As one can see in the figure, the HST-1 knot in its quiescent level is a small region of enhanced emission compared to the AGN elongated along the jet axis.
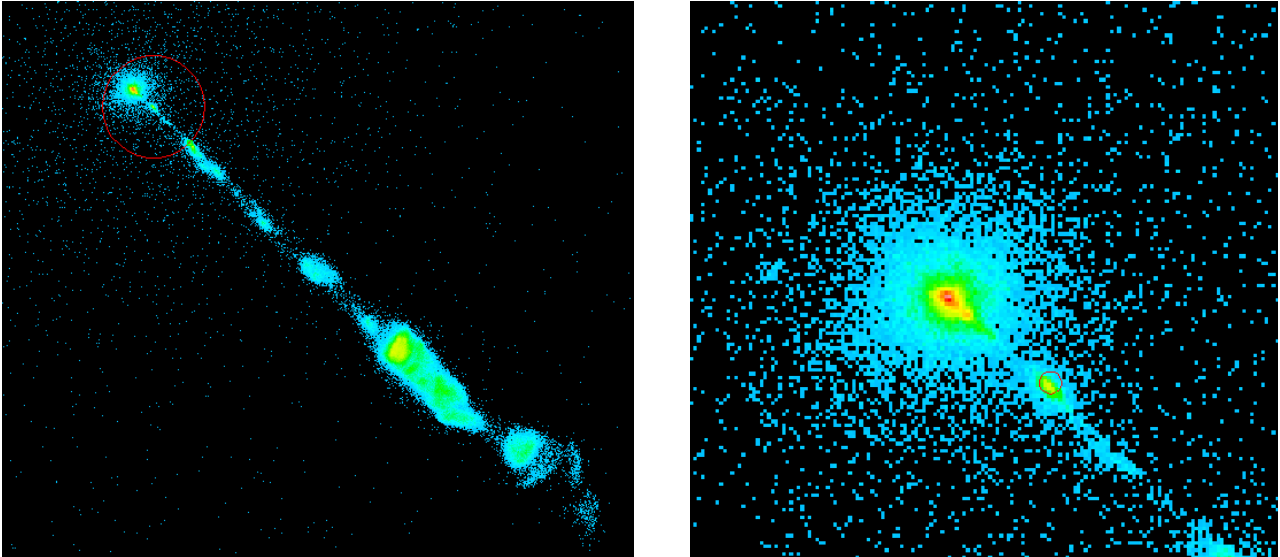
Figure 2 – *Image from file o5dc01byq_flt.fits of the M87 jet (left) and a zoom of the HST-1 knot next to the AGN (right) in 1999 May 17. The meaning of the red circles superimposed on the images will be explained later in the text.*

In 2001 July 30 the brightness of the HST-1 knot is four times over its quiescent level (see ref. [2]) and its dimensions have grown with respect to the ones in 1999 May 17 as illustrated in Figure 3.
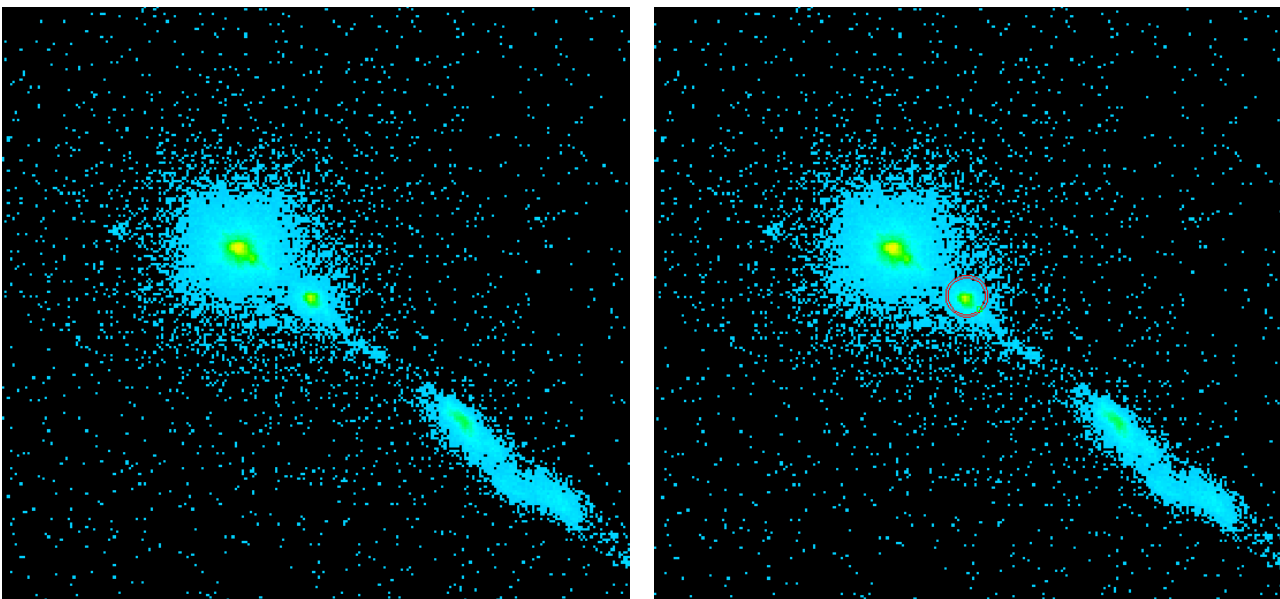
Figure 3 – *Image from file o6a351evq_flt.fits of the HST-1 knot in 2001 July 30. The red annulus superimposed on the image on the right has an outer radius of 8.25 pixels and a thickness of 1 pixel (see later in the text).*

Since the projection of the HST-1 knot on the sky plane in 2001 July 30 is circle-like shaped, coherently with the basic picture of an explosion process we will model the HST-1 outburst as a uniform bright sphere expanding at constant speed in all directions.

This model is further confirmed at subsequent epochs. For example, see Figure 4, the HST-1 knot is approximately a circle in 2003 July 27 when the last STIS images were obtained.
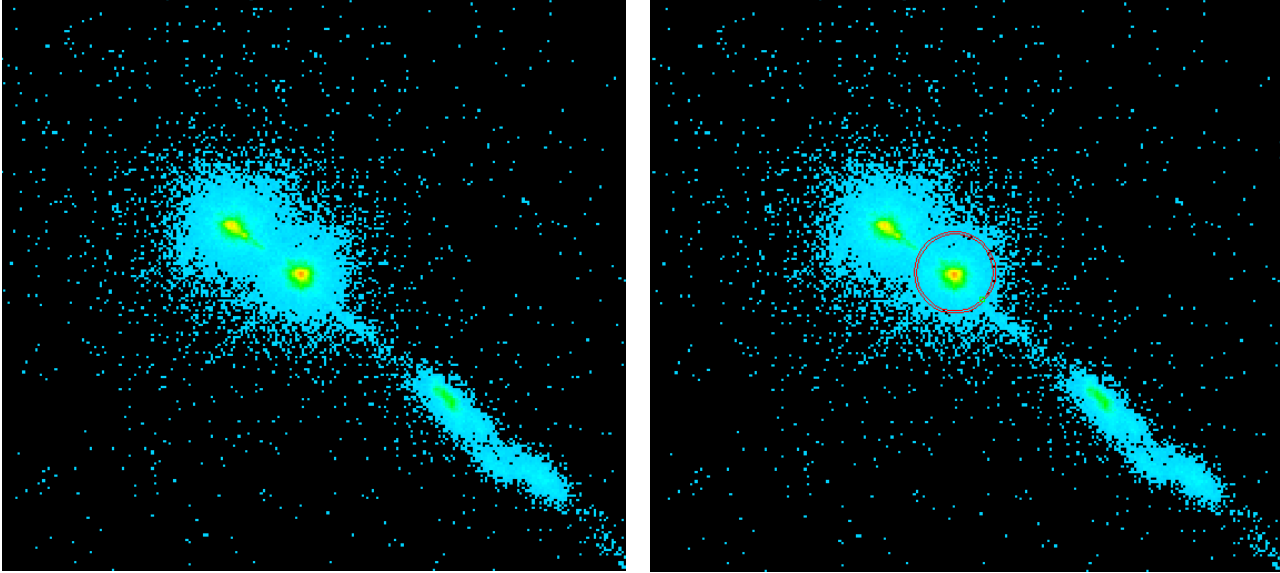
Figure 4 – *Image from file o6n712tiq_flt.fits of the HST-1 knot in 2003 July 27. The red annulus superimposed on the image on the right has an outer radius of 16.5 pixels and a thickness of 1 pixel (see later in the text).*

Now the circle resulting from the projection on the sky plane of a uniform luminous sphere expanding at constant relativistic velocity in all directions should be brighter in the center and fainter at the border. In fact, the fraction of emitted photons entering the telescope is affected by the speed of the source object and its direction of motion according to the law known as Doppler boosting. More precisely, the apparent brightness F_{app} in each point of the expanding luminous spherical surface depends on the real brightness F_{int} and the Doppler factor δ through the relation:

$$F_{app} = F_{int}\ \delta^n \tag{3}$$

where n is an empirical parameter and

$$\delta = \sqrt{1 - \frac{v^2}{c^2}}\ \frac{1}{1 - \frac{v}{c}\cos\theta} \tag{4}$$

Since the real brightness F_{int} and the real speed of expansion v are constant in each point of the surface, the apparent brightness F_{app} will only depend on the angle θ between the line of sight OT and the direction of motion OA (see Figure 1in section 2.1). It follows that the resulting projection on the sky plane will be a circle made up of concentric annuli, we have symmetry around the line of sight OT, with the faintest at the border where $\theta = 90°$ ($0° < \theta < 90°$ for the deformed sphere obtained when the relativistic correction for optical illusion is applied as we will see in the following section 2.3) and the brightest in the center where $\theta = 0°$.

For this reason, the two circumferences superimposed on the image o6a351evq in Figure 3 have been centered in the pixel (301, 856) where the software *fv 5.3* gives 1589.8 counts. This is the brightest pixel in the outburst region. The resulting annulus defining the border of the circle on the sky plane has a width of 1 pixel in agreement with the grain of the STIS images. Furthermore, the brightness of the border has been chosen in the range 13.1 ± 0.6 mean counts per pixel. This definition of brightness based on counts depends on the exposure time as illustrated in Table 1.

EXP	BORDER	FLUX
sec	counts per pixel	counts/s per pixel
558	11.6 ÷ 12.8	0.021 ÷ 0.023
580	12.1 ÷ 13.3	0.021 ÷ 0.023
600	12.5 ÷ 13.7	0.021 ÷ 0.023
640	13.4 ÷ 14.6	0.021 ÷ 0.023

Table 1 – *Brightness in counts per pixel defining the border of the outburst on the sky plane as a function of the exposure time. In the last column the corresponding brightness in counts/s per pixel is given.*

As one can see, all the different definitions given in Table 1 correspond to the same brightness when defined in counts/s per pixel (0.022 ± 0.001 counts/s per pixel). So, the brightness of the border in counts per pixel is uniquely defined allowing to compare properly all the images with different exposure times.

It should be noted that the choice of the value 0.022 ± 0.001 counts/s per pixel is an attempt to fit at best with the dimensions of the outburst avoiding in the meantime regions where the border of the circle on the sky plane is rather jagged. Furthermore, regions where the counts generated by the AGN can modify our measurement are avoided as well.

Now, the measurement on the image is performed as follows. We open the calibrated file o6a351evq by using the software *fv 5.3* provided by GSFC/NASA. For a better vision of the image in *logarithmic/Continuous/inv_spec* color, the minimum is set to 4 counts and the *Colorbar* is tuned properly. Then, by using the tool *Region Files*, we superimpose two circumferences of radius 7.5 and 6.5 pixels (physical pixels) respectively on the image. The two circumferences, one marked with plus and the other one with minus, are both centered in the point (301.5, 856.5) pixels.

An annulus 1-pixel thick results in this way. At this point, one can see in the entry *Mean Flux* that 17.3085 ± 1.38229 counts per pixel are measured in this annulus. Since this interval does not have any point in common with the interval 12.5 ÷ 13.7 counts per pixel, the annulus does not represent the border of the outburst on the sky plane for an exposure time of 600 s.

Instead for the annulus built with two circumferences of radius 8.0 and 7.0 pixels respectively, the interval 14.4854 ± 0.851214 counts per pixel intersects with the interval 12.5 ÷ 13.7 counts per pixel. So, this annulus has the right brightness to represent the outburst border. The same is true considering the annulus built with two circumferences of radius 8.5 and 7.5 pixels respectively. Even in this case, the brightness of the annulus 13.4177 ± 0.86517 counts per pixel has the right magnitude. Finally, the brightness of the annulus built with two circumferences of radius 9.0 and 8.0 pixels respectively is lower than 12.5 ÷ 13.7 counts per pixel since the software *fv 5.3* provides 10.9666 ± 0.760447 counts per pixel in the annulus. Therefore, this latter one cannot represent the outburst border.

In conclusion, we find that the dimensions of the outburst on the sky plane in 2001 July 30 are between 8.0 ÷ 8.5 pixels.

It should be noted that these dimensions have been found proceeding from the center of the circle by steps of 0.5 pixels. To explain this choice, we consider a measurement using a marked scale. For example, we measure the length of a pencil with a ruler. As illustrated in ref. [4], we must first place the end of the pencil opposite the zero of the ruler and then decide where the tip is positioned on the marked scale. We will see that the tip lies closer to a given mark that to either of its neighboring marks.

More precisely, if the tip is positioned closer to 80 mm than it is to 79 or 81 mm, we can conclude that the length of the pencil lies between 79.5 and 80.5 mm (80 ± 0.5 mm). No more precise reading is possible. Hence, the precision of the ruler is set to 0.5 mm.

Since the STIS images are made up of pixels, we can suppose by analogy that each mark on the scale now represents a pixel and so we can conclude that the precision of the measurements of the distances on the sky plane by the software *fv 5*.3 is 0.5 pixels. The use of shorter steps does not have any clear physical meaning.

Other three exposures at different times in 2001 July 30 are provided in files o6a351ewq, o6a351eyq and o6a351f0q. Following the same procedure developed for the analysis of the image in file o6a351evq, we find that the other three images give the same result for the dimensions of the outburst on the sky plane as illustrated in Table 2.

UT Date start date	UT Time start time	FILE _flt.fits	CENTER pixel	EXP sec	C PX counts	Y pixels
2001-07-30	23:18:40	o6a351evq	301.5 856.5	600	1589.8	8.0 ÷ 8.5
2001-07-30	23:29:28	o6a351ewq	321.5 846.5	600	1492.5	8.0 ÷ 8.5
2001-07-30	23:40:16	o6a351eyq	332.5 826.5	558	1553.7	8.0 ÷ 8.5
2001-07-30	23:50:22	o6a351f0q	311.5 836.5	600	1468.6	8.0 ÷ 8.5
2003-07-27	13:38:24	o6n712thq	291.5 826.5	640	7374.4	15.0 ÷ 16.5
2003-07-27	13:49:52	o6n712tiq	312.5 816.5	640	9436.2	14.0 ÷ 16.5
2003-07-27	14:01:20	o6n712tlq	323.5 795.5	640	8953.5	14.0 ÷ 15.5
2003-07-27	14:12:48	o6n712tnq	302.5 806.5	640	9453.2	15.0 ÷ 17.0

Table 2 – *Dimensions of the outburst on the sky plane (Y) in 2001 July 30 and 2003 July 27. The coordinates of the center of the circle on the sky plane (CENTER), the brightness of the pixel where it is located (C PX) and the exposure time (EXP) are also given.*

Finally, combining the results obtained from the analysis of the four images and their corresponding start times, we have that in 2001 July 30 at the mean time 23:34:41 UT the mean dimensions of the outburst on the sky plane are in the range 8.0 ÷ 8.5 pixels.

Such being the case, it follows immediately that the best estimate of the dimensions of the outburst in 2001 July 30 is the middle point 8.25 pixels.

This data will be used as a reference point in the calculations to determine the expansion speed of the explosion. In this way we do not need to know the instant when the outburst began and the size of its source.

Now we consider the images of the outburst in 2003 July 27. The best estimate for the maximum expansion of the outburst on the sky plane is the average of the single results obtained from the analysis of each image (see Table 2).

More precisely, $^{max}y_{av} = (16.5+16.5+15.5+17.0)/4 = 16.375$ pixels that rounded off to the precision used for each measurement gives $^{max}y_{av} = 16.5$ pixels. Similarly, we have that the best estimate for the minimum expansion is $^{min}y_{av} = (15.0+14.0+14.0+15.0)/4 = 14.5$ pixels. So, we are confident that the dimensions of the outburst lie in the range $14.5 \div 16.5$ pixels.

The probable range for the average size of the circle on the sky plane for each date covered by the STIS images after 2001 July 30 is given in Table 3.

UT DATE start date	AV UT start time	Y_{av} pixels	UT DATE start date	AV UT start time	Y_{av} pixels
2002-02-27	05:47:03	$10.0 \div 11.0$	2003-07-13	11:32:58	$14.0 \div 16.0$
2002-07-17	09:10:15	$11.0 \div 12.5$	2003-07-14	19:47:23	$14.5 \div 16.0$
2003-06-07	13:27:23	$13.5 \div 15.0$	2003-07-21	15:53:19	$14.5 \div 16.0$
2003-06-08	13:27:50	$13.5 \div 15.5$	2003-07-24	20:18:08	$15.0 \div 16.5$
2003-06-09	11:52:19	$13.5 \div 15.0$	2003-07-25	15:30:33	$14.5 \div 16.5$
2003-06-10	11:52:43	$13.5 \div 15.0$	2003-07-26	12:42:37	$15.0 \div 16.5$
2003-07-12	05:49:02	$14.0 \div 15.5$	2003-07-27	13:55:36	$14.5 \div 16.5$

Table 3 – *Dimensions of the outburst on the sky plane for each date covered by the STIS observations after 2001 July 30. The single results from the images with the same date are combined to give the probable range for the size of the circle on the sky plane (y_{av}). The average of the start times of the exposures (AV UT) is also given.*

By using this data and the results in section 2.1 we can now calculate the expansion speed of the explosion. In fact, the border of the circle on the sky plane in 2001 July 30 is at 8.25 pixels from the center, while in 2003 July 27 it is between $14.5 \div 16.5$ pixels. So, the outburst expanded on the sky plane of $14.5 - 8.25 = 6.25$ pixels min and $16.5 - 8.25 = 8.25$ pixels max. Since the plate scale of the images is equal to 0.02475 arcsec/pixel, it follows that:

$$y_{min} = 6.25 \, \text{pixels} \times \frac{0.02475"}{1 \, \text{pixel}} \times \frac{77 \, \text{pc}}{1"} \times \frac{3.26156 \, \text{ly}}{1 \, \text{pc}} = 38.8 \, \text{ly}$$

$$y_{max} = 8.25 \, \text{pixels} \times \frac{0.02475"}{1 \, \text{pixel}} \times \frac{77 \, \text{pc}}{1"} \times \frac{3.26156 \, \text{ly}}{1 \, \text{pc}} = 51.3 \, \text{ly}$$

where 1″ corresponds to 77 pc being the distance of M87 equal to 16.1 Mpc (see ref. [2]).

The distance on the sky plane in the range $38.8 \div 51.3$ ly has been covered in the interval of time between 23:34:41 UT of 2001 July 30 and 13:55:36 UT of 2003 July 27. This corresponds to an apparent time $\delta t_a = 1.989282$ y (sidereal years).

Considering this value for δt_a and putting $y_s = 51.3$ ly, we can verify that equation (2) is satisfied for $v/c = 0.99925$ ($v = 0.99925$ ly/y). Similarly, putting $\delta t_a = 1.989282$ y again and $y_s = 38.8$ ly, we can verify that equation (2) is satisfied for $v/c = 0.99869$ ($v = 0.99869$ ly/y).

To sum up, the expansion speed of the outburst between 2001 July 30 and 2003 July 27 is measured to be $v/c = 0.99897 \pm 0.00028$ ($v = 0.99897 \pm 0.00028$ ly/y).

Always taking as reference point the dimensions of the outburst on the sky plane in 2001 July 30 (8.25 pixels) and following the same procedure illustrated above, the expansion velocity of the explosion has been measured for the other dates covered by the STIS images. The results are shown in Table 4.

UT date	VELOCITY v/c	UT Date date	VELOCITY v/c
2002-02-27	0.99901 ± 0.00042	2003-07-13	0.99885 ± 0.00033
2002-07-17	0.99888 ± 0.00046	2003-07-14	0.99896 ± 0.00022
2003-06-07	0.99871 ± 0.00032	2003-07-21	0.99894 ± 0.00022
2003-06-08	0.99877 ± 0.00038	2003-07-24	0.99907 ± 0.00018
2003-06-09	0.99870 ± 0.00032	2003-07-25	0.99898 ± 0.00028
2003-06-10	0.99870 ± 0.00032	2003-07-26	0.99907 ± 0.00018
2003-07-12	0.99879 ± 0.00027	2003-07-27	0.99897 ± 0.00028

Table 4 – *Expansion velocity of the explosion for the dates covered by the STIS images.*

As one can immediately verify, all the results in Table 4 are consistent with each other. In fact, there is a common interval where all the measurements overlap. This means that the outburst expanded at constant speed in agreement with the picture of an explosion process in the vacuum.

At this point, we can combine all the measurements to give a single best estimate. This is the weighted average illustrated in ref. [4]:

$$v = \frac{\sum_i v_i w_i}{\sum_i w_i} \tag{5}$$

where the weight $w_i = \sigma_i^{-2}$ is the reciprocal square of the corresponding uncertainty σ_i associated to the measurement v_i obtained for each date covered by the STIS images. By using the data in Table 4 we find that $v/c = 0.99893$ is the best estimate.

Instead its associated uncertainty, see ref. [4] again, is:

$$\sigma = \frac{1}{\sqrt{\sum_i w_i}} \tag{6}$$

which gives $\sigma = 0.00007$ as a result.

In conclusion, we find that $v/c = 0.99893 \pm 0.00007$ is the best estimate with its associated uncertainty for the constant expansion speed of the outburst.

2.3 TOO BIG, TOO BRIGHT

The source of the outburst in its quiescent level is thought to be a spherical surface of radius r_s at rest. When the explosion occurs, this spherical surface begins to expand in all directions at constant speed. The section of the spherical surface that projected on the sky plane corresponds to the border of the circle seen in the STIS images moves at $v/c = 0.99893$ (see section 2.2) along the direction θ with respect to the line of sight OT. This angle is not 90° as one may think, but due to optical illusion we have $\theta = \arccos(0.99893) = 2.65°$ (see section 2.1).

Knowing that, we can derive the initial radius r_s of the source in its quiescent level. First, the start of the outburst has been constrained to 2000 February (see ref. [5] and ref. [6]) considering the ultraviolet radiation as generated by synchrotron emission. Hence, we can reasonably set the start time to 2000 February 15 at 00:00:00 UT. An apparent time $\delta t_a = 1.456463$ y must elapse from this instant until 23:34:41 UT of 2001 July 30 when the border of the circle on the sky plane is at 51.3 ly (8.25 pixels) from the center. This distance, as illustrated in Figure 5, is the projection on the y axis of OA.
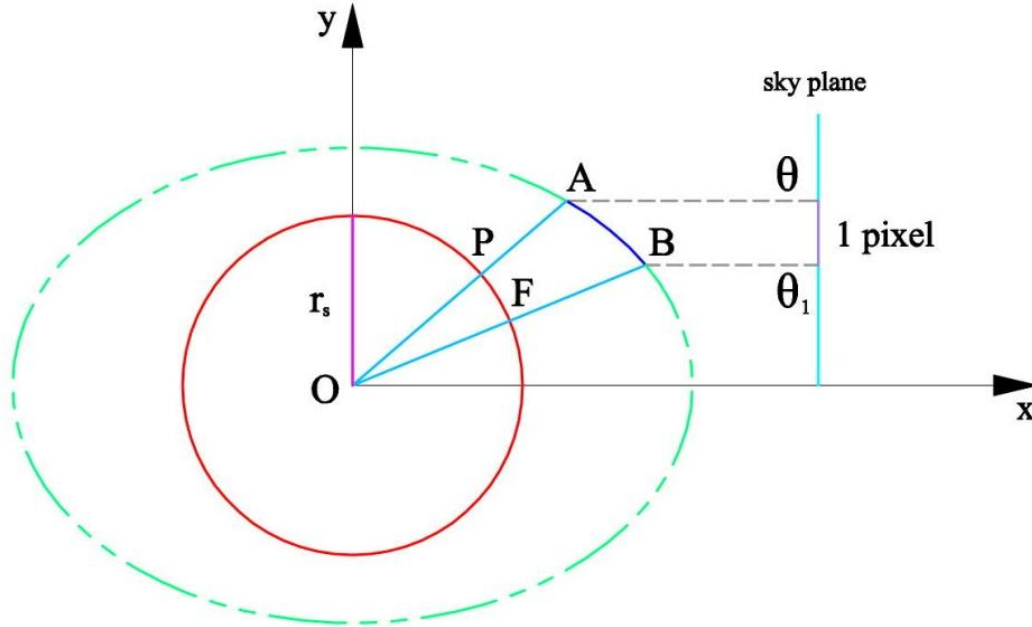
Figure 5 – *Section in the xy plane of the outburst source (red circle) and of the deformed sphere resulting from optical illusion (green dashed line). The figure is symmetric around the x axis oriented along the direction of the line of sight OT.*

Furthermore, in the same figure, we see that OA = OP + PA where OP is the initial radius r_s of the source in its quiescent level, while PA is the expansion r of the luminous spherical surface along the direction θ in the apparent interval of time δt_a elapsed between 2000 February 15 and 2001 July 30. Considering the real interval of time δt corresponding to this apparent interval of time, we can write by using equation (1):

$$\text{OA} \sin\theta = r_s \sin\theta + v \, \frac{\delta t_a}{1 - \dfrac{v}{c}\cos\theta} \sin\theta$$

From this relation it follows that:

$$r_s = \frac{OA \sin\theta}{\sin\theta} - v \frac{\delta t_a}{1 - \frac{v}{c}\cos\theta}$$

Since all the data is known, we have:

$$r_s = \frac{51.3}{\sin 2.65} - 0.99893 \frac{1.456463}{1 - 0.99893 \cos 2.65} = 429.1 \text{ ly}$$

Such a large initial radius for the outburst source seems to be very unlikely from a physical point of view. In fact, we consider the red circle of radius equal to 69 pixels (429.1 ly) superimposed on the left image in Figure 2. This circle centered in the brightest pixel of the HST-1 knot in its quiescent level is the projection on the sky plane of the outburst source. This means that the HST-1 knot, part of the M87 jet and probably the AGN are contained inside the spherical surface at rest representing the source before the explosion. Since the physical model accounting for the existence of a sphere of such dimensions and the mechanism triggering its expansion are completely unknown, it follows that the basic relativistic description of the outburst does not provide realistic results when going into details. This is further confirmed when the brightness of the expanding sphere is considered.

First, we determine the angular aperture of the annulus of outer radius equal to 8.25 pixels and inner radius equal to 7.25 pixels measured in 2001 July 30 (see Figure 3). As already seen, the direction corresponding to the outer radius is $\theta = 2.65°$, while the direction θ_1 corresponding to the inner radius is such that the projection of OB on the y axis is equal to 45.1 ly (7.25 pixels).

Now $OB = OF + FB$ where OF is the initial radius r_s of the source in its quiescent level, while FB is the expansion r_1 of the luminous spherical surface along the direction θ_1 in the apparent interval of time δt_a elapsed between 2000 February 15 and 2001 July 30 (see Figure 5). At this point, using again equation (1) we have:

$$OB \sin\theta_1 = r_s \sin\theta_1 + v \frac{\delta t_a}{1 - \frac{v}{c}\cos\theta_1} \sin\theta_1$$

or, substituting the known data,

$$45.1 = 429.1 \sin\theta_1 + 0.99893 \frac{1.456463}{1 - 0.99893 \cos\theta_1} \sin\theta_1$$

This equation, as one can verify by direct substitution, is solved for $\theta_1 = 1.99°$. Hence, the angular aperture corresponding to the border of the circle on the sky plane in 2001 July 30 is in the range $1.99° \div 2.65°$.

Instead the expansion of the section of the sphere that projected on the sky plane gives rise to this border 1 pixel thick can be defined as the average between PA and FB (see Figure 5). More precisely:

$$r_\theta = PA = v \frac{\delta t_a}{1 - \frac{v}{c}\cos\theta} = 0.99893 \frac{1.456463}{1 - 0.99893 \cos 2.65} = 680.4 \text{ ly}$$

$$r_{\theta_1} = FB = v \frac{\delta t_a}{1 - \frac{v}{c} \cos\theta_1} = 0.99893 \frac{1.456463}{1 - 0.99893 \cos 1.99} = 869.9 \text{ ly}$$

Combining these two results we have that in 2001 July 30 the section has expanded with respect to its rest position of:

$$r = \frac{PA + FB}{2} = \frac{680.4 + 869.9}{2} = 775.2 \text{ ly}$$

Now we determine the angular aperture of the annulus defining the border of the circle on the sky plane in 2003 July 27. Since the apparent time elapsed between 2000 February 15 and 2003 July 27 is equal to $\delta t_a = 3.445745$ y, it follows that the projection of OA on the sky plane (see Figure 5) is:

$$OA \sin\theta = (OP + PA) \sin\theta = \left(r_s + v \frac{\delta t_a}{1 - \frac{v}{c} \cos\theta} \right) \sin\theta =$$

$$= \left(429.1 + 0.99893 \frac{3.445745}{1 - 0.99893 \cos 2.65} \right) \sin 2.65 = 94.3 \text{ ly}$$

Since the annulus is 1 pixel thick, we have that the projection of OB on the sky plane (see Figure 5) is equal to $94.3 - 6.2 = 88.1$ ly. Following the same procedure illustrated previously, we find that the angular aperture of the border in 2003 July 27 is in the range $2.09° \div 2.65°$, while the corresponding section of the sphere has expanded with respect to its rest position of 1797.2 ly.

Then we can conclude that the angular aperture of the border of the circle on the sky plane remains the same during the expansion of the outburst except for a little discrepancy of the order of one tenth of degree ($1.99° \div 2.65°$ in 2001 July 30 and $2.09° \div 2.65°$ in 2003 July 27). So, from equation (4) it follows that the Doppler factor δ does not suffer any change from one epoch to the other. The same conclusion is obtained when all the preceding epochs covered by the STIS observations are analyzed.

Now we consider the brightest pixel in the outburst region where the circle on the sky plane has been centered to determine the real brightness F_{int} of this latter one. In 2001 July 30, by using the data in Table 2, we find that the apparent brightness F_{app0} of the central pixel in counts/s (per pixel is implied since we are considering a single pixel) is:

$$F_{app0} = \left(\frac{1589.8}{600} + \frac{1492.5}{600} + \frac{1553.7}{558} + \frac{1468.6}{600} \right) \frac{1}{4} = \frac{2.6 + 2.5 + 2.8 + 2.4}{4} = 2.6 \text{ counts/s}$$

$$\sigma = \sqrt{\frac{\sum_i (F_i - F_{app0})^2}{3}} = \sqrt{\frac{(2.6 - 2.6)^2 + (2.5 - 2.6)^2 + (2.8 - 2.6)^2 + (2.4 - 2.6)^2}{3}} = 0.2 \text{ counts/s}$$

Instead the angular aperture θ_0 corresponding to the central pixel is such that the projection of OD on the y axis is equal to 3.1 ly (0.5 pixels) as illustrated in Figure 6.
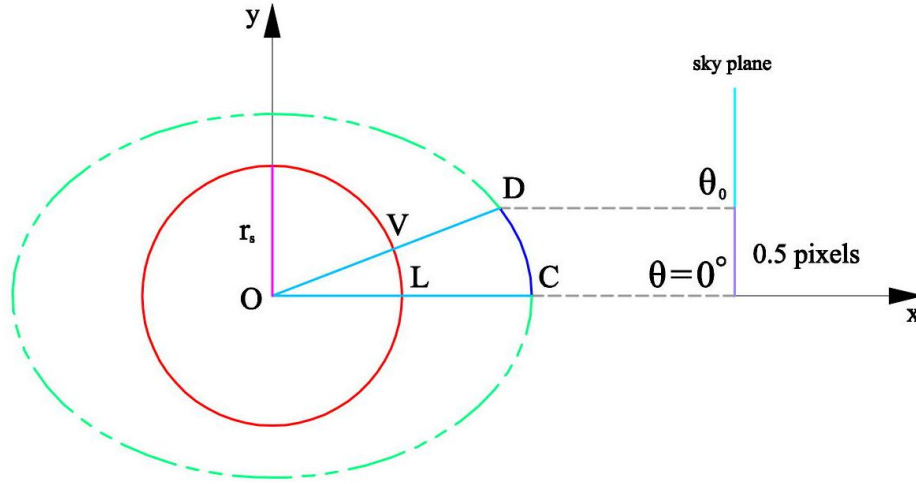
Figure 6 – *Section in the xy plane of the outburst source (red circle) and of the deformed sphere resulting from optical illusion (green dashed line). The angular aperture of the central pixel has been exaggerated for clarity purposes.*

Since OD = OV+VD, it follows that:

$$3.1 = 429.1 \sin\theta_0 + 0.99893 \, \frac{1.456463}{1 - 0.99893 \cos\theta_0} \, \sin\theta_0$$

The above equation, as one can verify by direct substitution, is solved for $\theta_0 = 0.10°$ and so the angular aperture corresponding to the central pixel in 2001 July 30 is in the range $-0.10° \div 0.10°$. Similarly, we find that the angular aperture corresponding to the central pixel in the subsequent epochs covered by the STIS images has a steady decrease. For simplicity, we will suppose in the following discussion that this quantity remains constant in time (conservative approximation).

Because the angular aperture is very small, the expansion of the section of the sphere corresponding to the central pixel will be calculated at $\theta = 0°$ only. As illustrated in Figure 6, the expansion r_0 in 2001 July 30 is:

$$r_0 = LC = 0.99893 \, \frac{1.456463}{1 - 0.99893 \cos 0} = 1359.7 \text{ ly}$$

In a similar way, the expansion r_0 is calculated for the other dates as shown in Table 5. From the data one can see that during its expansion the section of the sphere corresponding to the central pixel becomes brighter. In other words, F_{app0} increases while r_0 broadens out.

UT date	δt_a years	r ly	r_0 ly	F_{app0} counts/s
2000-02-15	0	0	0	0.3
2001-07-30	1.456463	775.2	1359.7	2.6 ± 0.2
2002-02-27	2.034847	1074.3	1899.7	3.2 ± 1.2
2003-07-27	3.445745	1797.2	3216.9	13.8 ± 1.5

Table 5 – *Expansion with respect to its rest position of the section of the sphere corresponding to the circle border (r) and to the central pixel (r_0). The brightness F_{app0} of the central pixel is also given.*

From its quiescent level at 0.3 counts/s in 2000 February 15, the brightness of the central pixel rises to 2.6 ± 0.2 counts/s in 2001 July 30 when the expansion of the corresponding section of the sphere is 1359.7 ly. In 2002 February 27 the brightness becomes higher reaching 3.2 ± 1.2 counts/s at an expansion of 1899.7 ly. A good fit of this data is obtained by the linear law:

$$F_{app0} = 0.3 + 1.92 \cdot 10^{-3}\, r_0 \tag{7}$$

Now we can derive F_{int} as a function of the expansion of the sphere with respect to its rest position along the direction $\theta = 0°$. In fact, combining equation (3) and equation (7) we have:

$$F_{int} = F_{app0}\, \delta_0^{-n} = \left(0.3 + 1.92 \cdot 10^{-3}\, r_0\right) \delta_0^{-n}$$

where the Doppler factor δ_0 is constant because the angular aperture does not depend on the expansion r_0 of the spherical surface as noticed previously.

Since we have supposed that the expanding luminous spherical surface is isotropic, it follows that F_{int} does not depend on θ. So, the behavior of F_{int} at the angle θ will be the same of the one determined at $\theta = 0°$. More precisely, it is:

$$F_{int} = \left(0.3 + 1.92 \cdot 10^{-3}\, r\right) \delta_0^{-n} \tag{8}$$

where r is the expansion of the sphere along any direction θ.

At this point, we can compare the apparent brightness of the border of the circle on the sky plane in 2001 July 30 with the one in 2003 July 27. In fact, using equation (3) and equation (8) we can write:

$$\frac{F_{app}^{03/07/27}}{F_{app}^{01/07/30}} = \frac{\left(0.3 + 1.92 \cdot 10^{-3}\, r_{03/07/27}\right) \delta_0^{-n}\ \delta^n}{\left(0.3 + 1.92 \cdot 10^{-3}\, r_{01/07/30}\right) \delta_0^{-n}\ \delta^n} = \frac{\left(0.3 + 1.92 \cdot 10^{-3}\, r_{03/07/27}\right)}{\left(0.3 + 1.92 \cdot 10^{-3}\, r_{01/07/30}\right)}$$

where also the Doppler factor δ is constant because the angular aperture of the border does not depend on the expansion r of the spherical surface as found previously. Using the data in Table 5 we have:

$$\frac{F_{app}^{03/07/27}}{F_{app}^{01/07/30}} = \frac{\left(0.3 + 1.92 \cdot 10^{-3}\, r_{03/07/27}\right)}{\left(0.3 + 1.92 \cdot 10^{-3}\, r_{01/07/30}\right)} = \frac{\left(0.3 + 1.92 \cdot 10^{-3} \times 1797.2\right)}{\left(0.3 + 1.92 \cdot 10^{-3} \times 775.2\right)} = 2.1$$

Hence, the relativistic model predicts that the brightness of the border of the circle on the sky plane in 2003 July 27 is $F_{app} = 0.022 \times 2.1 = 0.046$ counts/s per pixel where 0.022 counts/s per pixel is the apparent brightness of the border in 2001 July 30. Since the exposure time in 2003 July 27 is 640 s, we have $0.046 \times 640 = 29$ counts per pixel which is in stark contrast with the 14 counts per pixel observed in the STIS images (see Table 1).

In conclusion, by the relativistic analysis we obtain that the outburst source is too big and the border of the circle on the sky plane is too bright.

3. SUPERLUMINAL OUTBURST

The simple model for an explosion process used in the relativistic analysis of the STIS images is based on the hypotheses that the expansion is uniform in all directions and the brightness of the spherical surface is the same in each point. These suppositions derive from our common experience and so we can assume that we are dealing with a reasonable model. On the other hand, if it is also supposed that nothing can travel faster than light, one will fail to explain the dimensions of the outburst source and the brightness of the border of the circle on the sky plane as shown in the previous section. At this point, one can introduce a more sophisticated description to portray the explosion process increasing its complexity until agreement with the STIS observations is reached. However, that does not seem the only reasonable procedure. In fact, one can also maintain the initial hypotheses describing the explosion process and abolish the postulate that nothing can travel faster than light. This alternative procedure does not contradict special relativity simply because there is nothing to contradict. As one can verify, the equations of special relativity do not provide any real result when substituting $v > c$. Not being defined there, it follows that the superluminal world is not the application field of special relativity. Nothing else can be deduced for sure. So, faster than light motions are not necessarily forbidden, but just new physical laws shall be used.

Starting from this point of view, let us reanalyze the STIS images with a different approach. First, using the data in Table 3 and not applying any correction for optical illusion we immediately see that the apparent motion of the outburst on the sky plane is superluminal. So, we suppose that even the real motion of the expanding bright sphere is superluminal. Furthermore, we also suppose that the light emitted by superluminal matter travels faster than light. In fact, it is assumed that the emitted light reaches the observer before the matter itself. On these foundations a new mechanical model is built.

3.1 SUPERLUMINAL CORRECTION FOR OPTICAL ILLUSION

We consider superluminal matter travelling at constant speed $v > c$ and forming an angle θ with respect to the direction OT as illustrated in Figure 1. We suppose that the light emitted from the superluminal matter travels at v^n/c^{n-1} with $n \in \mathbb{N}$ and $n > 1$. At time t_1 a light ray leaves the superluminal matter from point O, while at time t_2 a second light ray leaves the superluminal matter from point A. Since OT = OH + HT, the first light ray reaches the observer in T at time:

$$t_{1a} = t_1 + \frac{D + v\delta t\cos\theta}{\frac{v^n}{c^{n-1}}}$$

where D is the length of HT.

We suppose that the separation of T from O is such that φ is small enough to have the two distances AT and HT equal, AT= HT = D. Hence, the second light ray reaches the observer in T at time:

$$t_{2a} = t_2 + \frac{D}{\frac{v^n}{c^{n-1}}}$$

In consequence, the observer in T will see the two light rays separated by an apparent interval of time:

$$\delta t_a = t_{2a} - t_{1a} = t_2 - t_1 - \frac{v\delta t\cos\theta}{\dfrac{v^n}{c^{n-1}}} = \delta t - \frac{\delta t\cos\theta}{\left(\dfrac{v}{c}\right)^{n-1}}$$

where $\delta t = t_2 - t_1$ is the temporal separation between the two emission processes.

So, we have that the relation between the real interval of time δt and the observed one δt_a is:

$$\delta t = \frac{\delta t_a}{1 - \dfrac{\cos\theta}{\left(\dfrac{v}{c}\right)^{n-1}}} \tag{9}$$

Now the projection y on the sky plane of the distance travelled by the superluminal matter in the real interval of time δt is (see Figure 1):

$$y = v\delta t\sin\theta = \frac{v\delta t_a\sin\theta}{1 - \dfrac{\cos\theta}{\left(\dfrac{v}{c}\right)^{n-1}}}$$

This quantity has its maximum for an angle θ such that $dy/d\theta = 0$. The derivative of y with respect to θ is:

$$\frac{dy}{d\theta} = \left(\frac{v}{c}\right)^{n-1} \frac{v\delta t_a\cos\theta}{\left(\dfrac{v}{c}\right)^{n-1} - \cos\theta} - \left(\frac{v}{c}\right)^{n-1} \frac{v\delta t_a\sin^2\theta}{\left[\left(\dfrac{v}{c}\right)^{n-1} - \cos\theta\right]^2} =$$

$$= v\delta t_a \left(\frac{v}{c}\right)^{n-1} \frac{\left(\dfrac{v}{c}\right)^{n-1}\cos\theta - \cos^2\theta - \sin^2\theta}{\left[\left(\dfrac{v}{c}\right)^{n-1} - \cos\theta\right]^2} = v\delta t_a \left(\frac{v}{c}\right)^{n-1} \frac{\left(\dfrac{v}{c}\right)^{n-1}\cos\theta - 1}{\left[\left(\dfrac{v}{c}\right)^{n-1} - \cos\theta\right]^2}$$

From the relation above we see that the projection y on the sky plane has its maximum, $dy/d\theta = 0$, when $\cos\theta = (v/c)^{1-n}$. Since at this angle $\sin\theta = [1 - (v/c)^{2-2n}]^{1/2}$, the maximum projection y_s on the sky plane of the distance travelled by the superluminal matter in the observed interval of time δt_a is:

$$y_s = v\delta t_a \frac{1}{\sqrt{1 - \left(\dfrac{v}{c}\right)^{2-2n}}} \tag{10}$$

The relations derived in this section will be used to correct for superluminal optical illusion the data provided by the STIS images.

3.2 OUTBURST SUPERLUMINAL SPEED

In this section, not having any indication on the speed of the UV radiation coming from the M87 jet, we will suppose for example that the light travels at v^{10}/c^9 where v is the superluminal speed of the emitting matter. In this way, the images are not the result of the superposition of angular sectors seen at different times as suggested by the relativistic model. Instead, each angular sector of the expanding sphere is seen at the same time being the correction for optical illusion negligible in this case.

Now we reconsider the data in section 2.2 derived from the relativistic analysis of the STIS images. As we have seen, the outburst expanded of $38.8 \div 51.3$ ly on the sky plane from 2001 July 30 to 2003 July 27. Since it is supposed that the expansion speed v of the outburst is the same in all directions, we can use equation (10) to correct for optical illusion.

More precisely, substituting $y_s = 51.3$ ly and $\delta t_a = 1.989282$ y the equation is satisfied for v/c = 25.8 (v = 25.8 ly/y), while for $y_s = 38.8$ ly the equation is satisfied when v/c = 19.6 (v = 19.6 ly/y). So, the superluminal expansion speed of the outburst between 2001 July 30 and 2003 July 27 is measured to be v/c = 22.7 ± 3.1 (v = 22.7 ± 3.1 ly/y).

Following the same procedure illustrated above, the superluminal expansion velocity of the outburst has been measured for the other dates covered by the STIS images. Again, the dimensions of the outburst on the sky plane in 2001 July 30 (8.25 pixels) have been taken as reference point and the data in Table 3 has been used. The results are shown in Table 6.

As one can immediately verify, all the measurements are consistent with each other implying that the outburst expanded at constant superluminal speed in agreement with the picture of an explosion process in the vacuum.

In conclusion, combining all the measurements in a single result by equation (5) and equation (6), we get that v/c = 21.8 ± 0.7 (v = 21.8 ± 0.7 ly/y) is the best estimate with its associated uncertainty for the superluminal speed.

UT date	VELOCITY v/c	UT date	VELOCITY v/c
27/02/2002	24.2 ± 5.4	13/07/2003	21.5 ± 3.2
17/07/2002	22.6 ± 4.8	14/07/2003	22.3 ± 2.4
07/06/2003	20.1 ± 2.5	21/07/2003	22.1 ± 2.4
08/06/2003	20.9 ± 3.4	24/07/2003	23.5 ± 2.4
09/06/2003	20.1 ± 2.5	25/07/2003	22.7 ± 3.1
10/06/2003	20.0 ± 2.5	26/07/2003	23.5 ± 2.3
12/07/2003	20.7 ± 2.4	27/07/2003	22.7 ± 3.1

Table 6 – *Superluminal expansion velocity of the outburst for the dates covered by the STIS images.*

3.3 FAINT BORDER ORIGINATING IN THE HST-1 KNOT

In the superluminal case the section of the expanding spherical surface that projected on the sky plane corresponds to the border of the circle seen in the STIS images moves at v/c = 21.8 (see section 3.2) along the direction $\theta = \arccos(21.8)^{-9} = 90°$ (see section 3.1) with respect to the line of sight OT.

When an apparent time $\delta t_a = 1.456463$ y has elapsed from the start of the outburst to 23:34:41 of 2001 July 30, the border of the circle on the sky plane is at 51.3 ly (8.25 pixels) from the center (see section 2.2). This distance, as illustrated in Figure 7, is the projection on the y axis of OA.
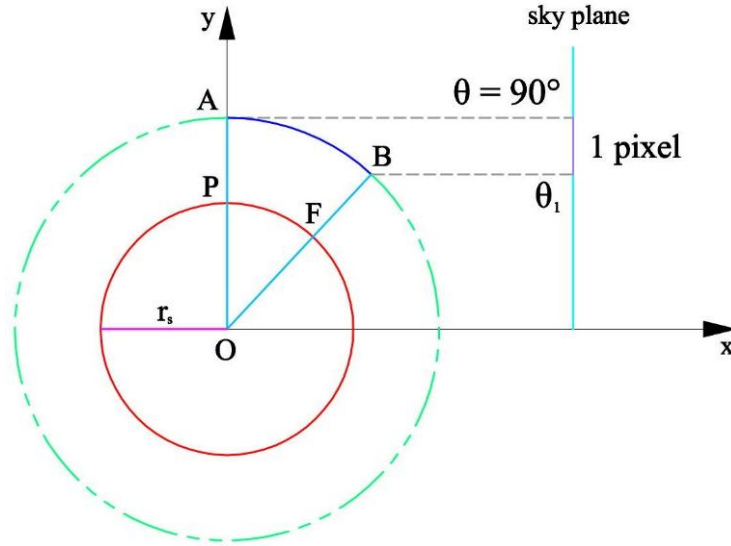
Figure 7 – *Section in the xy plane of the outburst source (red circle) and of the sphere resulting from the expansion caused by the explosion process (green dashed line). The figure is symmetric around the x axis oriented along the direction of the line of sight OT.*

Since OA = OP + PA where OP is the initial radius r_s of the source in its quiescent level and PA is the expansion r of the luminous spherical surface along the direction θ in the apparent interval of time δt_a elapsed between 2000 February 15 and 2001 July 30, we can write by using equation (9):

$$\text{OA} \sin\theta = r_s \sin\theta + v \, \frac{\delta t_a}{1 - \dfrac{\cos\theta}{\left(\dfrac{v}{c}\right)^{n-1}}} \, \sin\theta$$

Solving for r_s and substituting the known data ($\theta = 90°$), we have:

$$r_s = 51.3 - 21.8 \times 1.456463 = 19.5\,\text{ly}$$

Differently from the relativistic case, such initial radius for the outburst source is more reasonable from a physical point of view. In fact, the circle of radius equal to 3 pixels (19.5 ly) superimposed on the right image in Figure 2 does not exceed the dimensions of the HST-1 knot. This means that the spherical surface at rest representing the outburst source before the explosion is located inside the HST-1 knot. The origin of the explosion is then the HST-1 knot itself as claimed in the literature on the subject and, on top of that, as clearly seen in the STIS images.

Now we consider the brightness of the annulus of outer radius equal to 8.25 pixels and inner radius equal to 7.25 pixels measured in 2001 July 30 (see Figure 3). The direction corresponding to the outer radius is $\theta = 90°$, while the direction θ_1 corresponding to the inner radius is such that the projection of OB on the y axis is equal to 45.1 ly (7.25 pixels). Since OB = OF + FB where OF is

the initial radius r_s of the source in its quiescent level and FB is the expansion r_1 of the luminous spherical surface along the direction θ_1 in the apparent interval of time δt_a (see Figure 7), we have:

$$\text{OB}\sin\theta_1 = r_s\sin\theta_1 + v\,\frac{\delta t_a}{1 - \dfrac{\cos\theta_1}{\left(\dfrac{v}{c}\right)^{n-1}}}\,\sin\theta_1$$

Substituting the known data, we get:

$$45.1 = 19.5\sin\theta_1 + 21.8\,\frac{1.456463}{1 - \dfrac{\cos\theta_1}{21.8^9}}\,\sin\theta_1$$

Because the solution of this equation is given by $\theta_1 = 61.6°$, the angular aperture of the border in 2001 July 30 is roughly in the range $62° \div 90°$.

Instead the expansion of the sphere with respect to its rest position is:

$$r = v\,\frac{\delta t_a}{1 - \dfrac{\cos\theta}{\left(\dfrac{v}{c}\right)^{n-1}}} = 21.8 \times 1.456463 = 31.7\ \text{ly}$$

The expansion calculated for $\theta = 90°$ is the same for each angle when δt_a is given. Unlike the relativistic case, we see on the sky plane the projection of a sphere and not the projection of its sectors seen at different expansions according to the angle considered.

Now we determine the projection of OA on the sky plane (see Figure 7) in 2003 July 27 when an apparent time $\delta t_a = 3.445745$ y has elapsed from 2000 February 15. Given $\theta = 90°$, we have:

$$\text{OA}\sin\theta = (\text{OP}+\text{PA})\sin\theta = r_s\sin\theta + v\,\frac{\delta t_a}{1 - \dfrac{\cos\theta}{\left(\dfrac{v}{c}\right)^{n-1}}}\,\sin\theta = 19.5 + 21.8 \times 3.445745 = 94.6\ \text{ly}$$

The projection of OB on the sky plane (see Figure 7) is equal to $94.6 - 6.2 = 88.4$ ly instead. Following the same procedure illustrated previously, we find that the angular aperture of the annulus defining the border of the circle on the sky plane in 2003 July 27 is roughly in the range $69° \div 90°$, while the sphere has expanded of 75.1 ly with respect to its rest position. At this point, we determine the angular aperture θ_0 corresponding to the central pixel in 2001 July 30. As illustrated in figure 8, the projection of OD on the y axis must be equal to 3.1 ly (0.5 pixels). Since OD = OV+VD, it follows that:

$$3.1 = 19.5\sin\theta_0 + 21.8\,\frac{1.456463}{1 - \dfrac{\cos\theta_0}{\left(\dfrac{v}{c}\right)^{n-1}}}\,\sin\theta_0$$

The solution of the above equation is found to be $\theta_0 = 3.5°$ and so the angular aperture corresponding to the central pixel in 2001 July 30 is in the range $-3.5° \div 3.5°$. Similarly, you can verify that the angular aperture corresponding to the central pixel in the subsequent epochs covered by the STIS images has a steady decrease falling to $-1.9° \div 1.9°$ in 2003 July 27. For simplicity, we will suppose in the following discussion that the angular aperture remains constant during the expansion (conservative approximation).
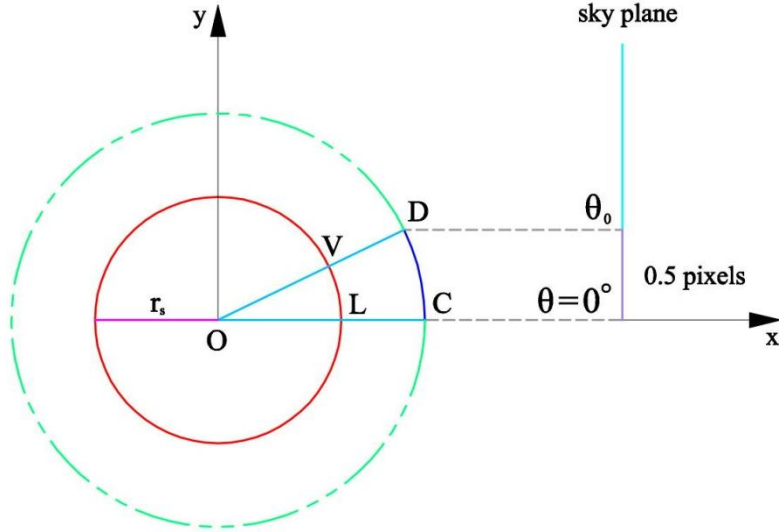
Figure 8 – *Section in the xy plane of the outburst source (red circle) and of the sphere during its superluminal expansion (green dashed line). The angular aperture of the central pixel has been exaggerated for clarity purposes.*

The apparent brightness F_{app0} of the central pixel is equal to 2.6 ± 0.2 counts in 2001 July 30 when the sphere has expanded of 31.7 ly with respect to its rest position. Instead in 2003 July 27 the brightness rises to 13.8 ± 1.5 counts in the central pixel (see Table 5) at an expansion of 75.1 ly.

Now we suppose that the Doppler boosting continue to be present also in the superluminal case. Then equation (3) will be used where the Doppler factor δ, different from the relativistic one, is such that it decreases going from 0° to 90°. So, the superluminal light emitted along the line of sight OT is enhanced, while the superluminal light emitted at right angles is darkened. This agrees with the STIS observations where the center of the circle on the sky plane is brighter than its border. Without the superluminal Doppler boosting we should see a circle of uniform brightness because F_{int} is constant throughout the luminous spherical surface and the pixels of the image are of constant size. F_{int} only depends on the expansion of the luminous sphere. Since the expansion of the angular sectors for each date is the same in the interval $0° \div 90°$ as already noticed, we can use the values of F_{int} at 0° for the ones at 90°.

At this point, we can compare the apparent brightness of the border in 2001 July 30 with the one in 2003 July 27. Using equation (3) it follows that:

$$\frac{F_{app90}^{03/07/27}}{F_{app90}^{01/07/30}} = \frac{F_{int90}^{03/07/27} \, \delta_{69 \div 90}^{n}}{F_{int90}^{01/07/30} \, \delta_{62 \div 90}^{n}} = \frac{F_{int0}^{03/07/27} \, \delta_{69 \div 90}^{n}}{F_{int0}^{01/07/30} \, \delta_{62 \div 90}^{n}} = \frac{F_{app0}^{03/07/27} \, \delta_0^{-n} \, \delta_{69 \div 90}^{n}}{F_{app0}^{01/07/30} \, \delta_0^{-n} \, \delta_{62 \div 90}^{n}} = \frac{13.8 \, \delta_{69 \div 90}^{n}}{2.6 \, \delta_{62 \div 90}^{n}} = 5.3 \, \frac{\delta_{69 \div 90}^{n}}{\delta_{62 \div 90}^{n}}$$

In this way we see that the superluminal model can account for the constant apparent brightness of the border of the circle on the sky plane for each epoch covered by the STIS images. In fact, the superluminal Doppler factor δ in 2003 July 27 is smaller than the one in 2001 July 30 because the angular interval covered by this latter one is greater of about 7°. Hence, a ratio equal to 1 can be obtained in the relation written above in agreement with the observations.

In conclusion, the superluminal model predicts that the outburst source is contained in the HST-1 knot and the border of the circle on the sky plane maintains the same brightness during the expansion.

4. SUPERLUMINAL OBSERVATIONS

In section 3.3 we have seen that the features of the outburst, source dimensions and brightness of the border of the circle on the sky plane, are better explained considering a superluminal expansion. Obviously, this is not intended to be a claim of such kind of discovery since the basic and reasonable model used to describe the explosion process could be too simplified. However, it is not the first time where superluminal motion has been observed.

For example, the proper motion of 12 features within the first 6" of the M87 jet was measured in the optical waveband. Of these, 10 appear to be superluminal with eight having apparent speeds in the range 4c ÷ 6c. The most natural explanation given to account for the observed superluminal speeds is that they are due to bulk relativistic flow in the context of the relativistic jet model. The strongest constrain on the bulk flow speed and line-of-sight angle for the jet results from the largest speeds observed which are equal to about 6c. Hence, assuming that the flow velocity is directed parallel to the jet axis, the relativistic jet model requires a bulk flow with Lorentz factor $\gamma \geq 6$ and a jet orientation within θ ≤ 19° (see ref. [7]). Instead for a jet orientation θ > 19° the observed apparent motions corrected for relativistic optical illusion continue to show superluminal behavior.

Now we consider the available estimates of the jet orientation. For example, measurements of the M87 jet in the radio waveband revealed a bright and linear feature across the jet in knot A. It is reasonably assumed that this linear feature is a two-dimensional structure seen in projection: a filament wrapped around the jet or a disk. After a detailed analysis of the appearance of this structure on the sky plane, a jet orientation θ = 42.5° ± 4.5° to the line of sight has been derived (see ref. [8]). A value greater than 19° is also confirmed by further studies in the radio waveband of superluminal features in the HST-1 knot. More precisely, observations between 2005 December and 2006 February revealed that the feature HST1c split into two roughly equally bright features: a faster than light moving component (c_1; 4.3c ± 0.7c) and a slower than light moving trailing feature (c_2; 0.47c ± 0.39c). Instead the apparent point of origin of the superluminal ejections, the HST1d feature, remained basically stationary from the core between the two years of radio observations. By studying the kinematics of the superluminal radio components, in particular the 4.3c motion in c_1, a jet orientation θ = 26° ± 4° to the line of sight has been derived (see ref. [9]). Then it follows that the apparent superluminal motions observed in the optical waveband (see ref. [7]) are the result of matter travelling faster than light since the jet orientation θ is greater than 19°. However, even if the procedures used to determine the jet orientation are correct, the possibility that we are really observing superluminal motions does not deserve a little consideration in the literature.

Conversely, in the presence of superluminal observations, suitable additional effects such as instrumentation failure, additional variables to put into the model or unknown physical processes

are introduced to restore subluminality. Obviously, this procedure cannot be considered incorrect, but it should be used with caution to avoid the risk of twisting the reality.

An example of instrumentation failure introduced to restore subluminality is provided by the superluminal neutrinos observed in the OPERA experiment.

The first version of the OPERA data was released on the 22nd of September 2011, but a few months later the experimenters retracted their original results after further analysis. In fact, proper measurements of the time delay in the 8.3 km optical fiber between the ESAT GPS 1PPS output and the OPERA Master Clock output were made in December 2011. A value 73.2 ns larger than the one determined in 2006 and 2007 was found. The conclusion of the investigation revealed that the difference originated from an optical cable not properly connected. So, it was immediately inferred that the optical cable connection failed before the period 2009-2011 when faster than light motions were detected and not, for example, some day before the new measurements of the time delay carried out in December 2011.

This particularly bizarre method to derive results reminds the one relying on missing transverse momentum used in particle identification. As explained in ref. [10], momentum conservation, an elementary law, loosely speaking states that the debris after a collision is supposed to fly off in all directions, much as a snowball slammed into a wall will not just splash upwards or to the right. Such an asymmetry is occasionally observed in the collisions, and particle physicists conclude that a rare particle, such as a neutrino, went off undetected and kept the momentum balance. If the situation does not allow a neutrino going off, naturally, the door is open for further interpretation. An essential element of detection of the W boson relies on such missing transverse momentum. However, such an interpretation opens the floodgates for any kind of fanciful speculation, while in the extensively complicated collision there are plenty of reasons why the momentum could be missing: detector malfunction, interaction with the rest of the particles in the beam, with the beam tube, secondary interactions, lack of theoretical understanding of the multitude of processes involved or simply nasty little details one has not thought of before. All this is negligible according to conventional wisdom, but who knows? Once you interpret the deficit of transverse momentum, the methodological problem is that you actually get evidence from something which is missing, that is, seeing by non-seeing. Unfortunately, the subtle but infinite potential to fool oneself is one of the grave absurdities physicists (and even philosophers) never reflect on. And of course, it is impossible to separate theoretical assumption from (non-) observation.

However, in the OPERA superluminal neutrino case there is not any need to follow the seeing by non-seeing procedure to get results. In fact, additional independent information has been provided by studying cosmic muon events in delayed coincidence in the OPERA and LVD detectors taken from August 2007 to March 2012.

A quantitative analysis based on high school level physics and a detailed discussion of this further data, along with the proper references, can be found in Appendix C of ref. [11] and so it will not be repeated here. As a result, the study of the cosmic muon events revealed that the timing system of the OPERA detector worked correctly during the 2009-2011 neutrino data taking. This means that the muonic neutrinos really travelled faster than light as correctly shown in the first version of the OPERA data.

There are also updated results obtained from new measurements of the muonic neutrino velocity. For example, we analyze the time distribution δt illustrated in figure 9 of the 25 events measured in the ICARUS experiment (see ref. [12]).
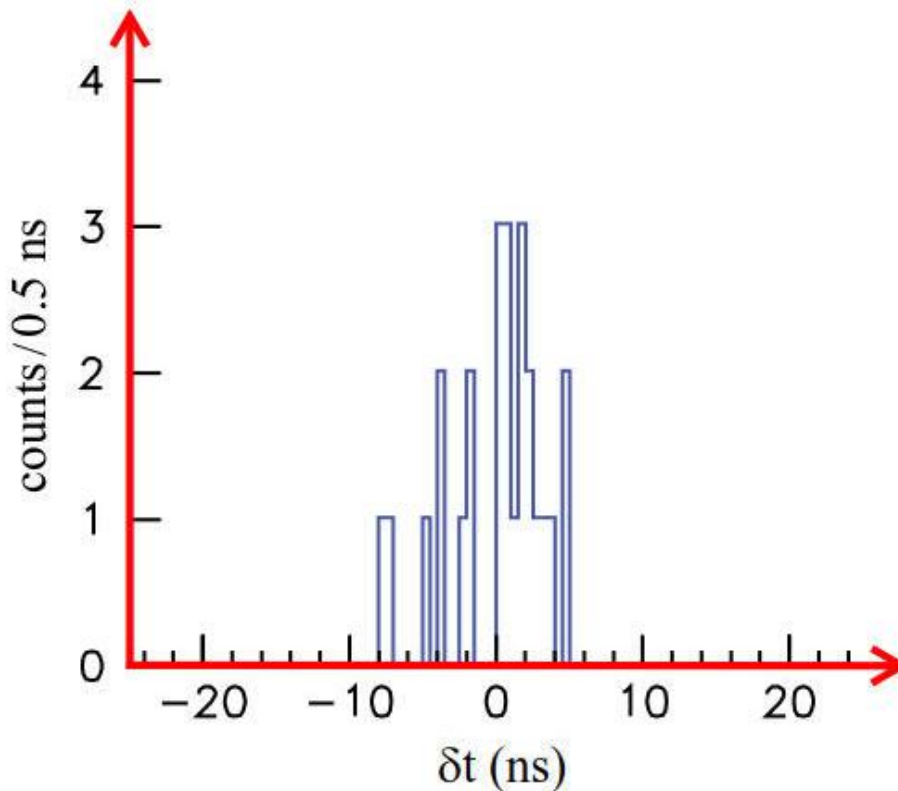
Figure 9 – *Distribution for δt = tof$_c$– tof$_v$ of the 25 events in ICARUS T600.*

The time distribution is defined as δt = tof$_c$ – tof$_v$ where tof$_c$ is the time taken by a muonic neutrino travelling at the speed of light to cover the distance d = 731221.95 m, tof$_c$ = 2439096.08 ns, while tof$_v$ is the time taken by a muonic neutrino travelling at a speed different from that of light to cover the same distance. When the muonic neutrino travels slower than light the time difference δt is negative, it takes more time to cover the distance d, while for superluminal velocities the time difference δt is positive, it takes less time to cover the distance d. From figure 9 one can see that for 8 events is δt < 0 and for 17 events is δt > 0. In other words, 8 muonic neutrinos have travelled slower than light and 17 muonic neutrinos have travelled faster than light.

Since subluminal motions are found in the data (8 events), it has been deduced that the ICARUS experiment does not support superluminal velocities although these latter ones are found in the data as well (17 events). Clearly this conclusion is consistent if and only if one supposes that the positive time differences δt have no physical meaning and so they are a mistake. That is very similar to the following situation.

To measure the rest mass of an object, this latter one is hung to a spring. From the stretching of the spring, by a suitable graduated scale, the rest mass of the object is derived (see figure 10). This kind of measurement is repeated several times and in some occasions the spring is compressed instead of being stretched. Obviously, in these latter cases the graduated scale will give a negative value for the rest mass of the object. Since negative values do not have any physical meaning, they will be rejected instead of being used to calculate the mass of the object. Conversely the result will not be correct. In fact, for example, if two measurements give 500 kg and the other two give −500 kg, one could even find that the best estimate (the average) for the weight of a steel ball 0.5 m in diameter is 0 kg.
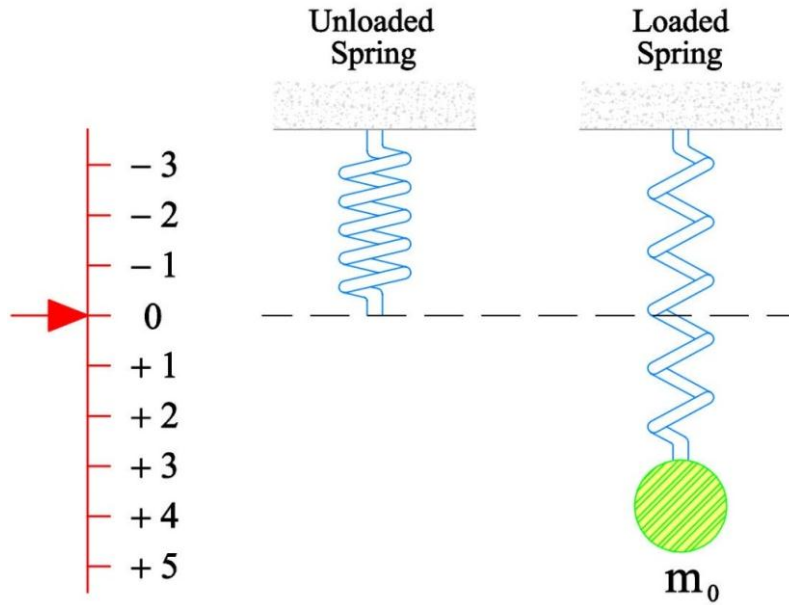
Figure 10 – *Measurement of the rest mass m_0 by the stretching of a loaded spring.*

Now the outcome of the ICARUS experiment, $\delta t = 0.10 \pm 0.67$ ns, was obtained by considering both positive and negative values of the time difference δt, in our analogy both positive and negative values of the rest mass. At this point, one cannot use the ICARUS result to claim the nonexistence of superluminal motions because, in the meantime, one is also claiming that this result is incorrect. Instead, if nothing can travel faster than light, the accurate value should be obtained calculating the mean and the standard deviation of the mean by just using the 8 subluminal events in Figure 9. The 17 superluminal events are not considered being the unphysical ones. According to the data reported in Table 7 we have $\delta t = -3.9 \pm 2.3$ ns.

δt (ns)	
−1.5	−3.5
−1.5	−4.5
−2.0	−7.0
−3.5	−7.5

Table 7 – *Time difference δt for the 8 subluminal events in the ICARUS T600. Conservatively, the minimum value in each 0.5-ns interval has been considered.*

Substituting this value in the relation $v/c - 1 = \delta t / (tof_c - \delta t)$ we get $v/c = 0.9999984 \pm 0.0000009$ as a result. Finally, deriving the muonic neutrino rest mass from the equation $m_0 c^2 = E\,(1 - v^2/c^2)^{1/2}$ provided by special relativity (conservatively E = 10 GeV) we obtain $m_0 c^2 = 17 \pm 5$ MeV.

This value is in sharp disagreement with the current accepted value $m_0 c^2 < 170$ keV. The same conclusion is obtained when considering the data from BOREXINO, OPERA (updated) and LVD experiments (see ref. [13], [14], [15] respectively).

At this point, the failure of special relativity does not arise from the theory itself but from its commonly accepted interpretations. In fact, not following these latter ones and consequently

viewing the observed 17 superluminal events in Figure 9 as real physical data, clearly the result of the ICARUS experiment $\delta t = 0.10 \pm 0.64$ ns can be considered correct.

So, using the same procedure illustrated above we find that the muonic neutrino rest mass is estimated to be $m_0 c^2 < 7$ MeV in agreement with the current accepted value.

Obviously, only the values of the time distribution δt in the range $-0.54 \div 0$ ns have been used in the relativistic equation to calculate the muonic neutrino rest mass because the remaining values of δt in the range $0 \div 0.74$ ns give an imaginary result. Hence, it follows that another equation deriving from another physics must be used to calculate the rest mass of superluminal neutrinos. This new physics could have some similarities with the fundamental structure of special relativity but surely it cannot be a copy of this latter one. One cannot translate into the superluminal world the theoretical framework of a theory failing to describe the behavior of faster-than-light objects. More details on this topic can be found in ref. [11] along with the exposition of a possible superluminal physics.

In conclusion, we have seen in this section that the refusal of superluminal motions in physics seems to be a bias. In fact, we have even found ironically that they are needed to confirm the predictions of special relativity as shown by the updated time-of-flight measurements of ICARUS, BOREXINO, OPERA and LVD experiments.

5. AT THE CENTER OF THE UNIVERSE

5.1 THE PARADOX OF THE CLOCKS

We begin discussing the paradox of the clocks. This paradox is the simplest form of the well-known twin paradox.

We consider a clock A at rest in the origin O of the inertial reference frame R and a clock B moving along the x axis at constant speed v as illustrated in Figure 11.
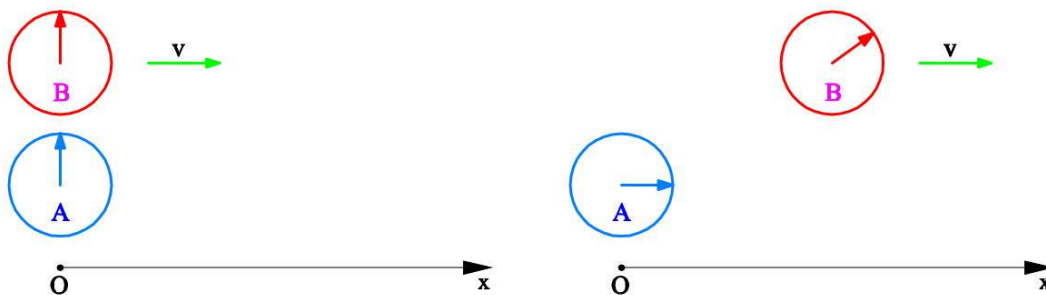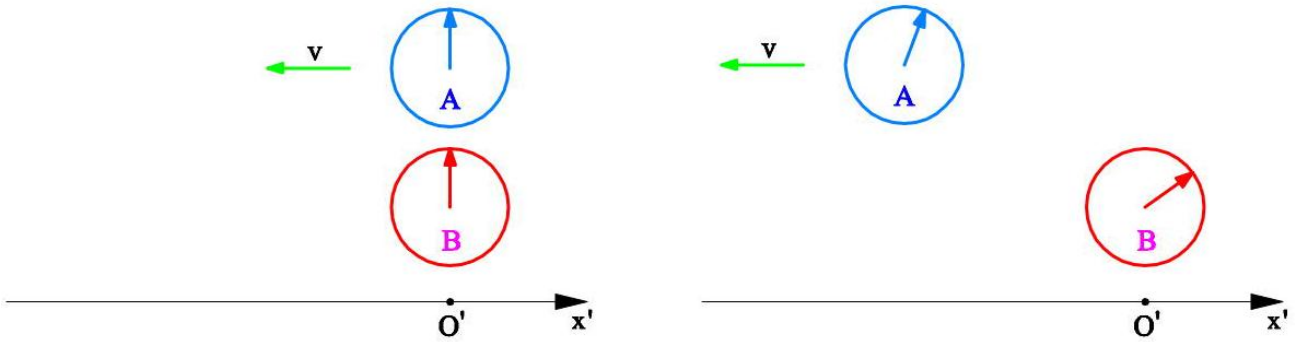

Figure 11 – *Clock A at rest in the origin O of the inertial reference frame R and clock B moving along the x axis at constant speed v. The reading of the two clocks when superimposed in the origin is zero.*

When the clock B is in the origin O along with the clock A, both clocks are set to read zero. Instead when the moving clock B is in the new position $x = v\,t$, this latter one will read a time $t' < t$ where t is the time registered by clock A.

In fact, we suppose that the clock B is at rest in the origin O' of the inertial reference frame R' moving at constant speed v along the x axis of the inertial reference frame R. Using the Lorentz transformation from R to R' we get that the time registered by clock B is:

$$t' = \frac{1}{\sqrt{1 - \dfrac{v^2}{c^2}}} \left(t - \frac{v\,x}{c^2} \right) = \frac{t}{\sqrt{1 - \dfrac{v^2}{c^2}}} \left(1 - \frac{v^2}{c^2} \right) = t\,\sqrt{1 - \frac{v^2}{c^2}} \tag{11}$$

Now we think of the same situation from the point of view of the observer in R'. In this case, we consider the clock B at rest in the origin O' of the inertial reference frame R' and the clock A moving along the x' axis at constant speed $-v$ as illustrated in Figure 12.

Figure 12 – *Clock B at rest in the origin O' of the inertial reference frame R' and clock A moving along the x' axis at constant speed − v. The reading of the two clocks when superimposed in the origin is zero.*

When the clock A is in the origin O' along with the clock B, both clocks are set to read zero. Instead when the moving clock A is in the new position $x' = -v\,t'$, this latter one will read a time $t < t'$ where t' is the time registered by clock B.

In fact, using the Lorentz transformation from R' to R we get that the time registered by clock A is:

$$t = \frac{1}{\sqrt{1 - \dfrac{v^2}{c^2}}} \left(t' + \frac{v\,x'}{c^2} \right) = \frac{t'}{\sqrt{1 - \dfrac{v^2}{c^2}}} \left(1 - \frac{v^2}{c^2} \right) = t'\,\sqrt{1 - \frac{v^2}{c^2}} \tag{12}$$

Since the time flows forward at constant rate both in R and R', then there will be a one to one correspondence between the time t and the time t'. More precisely, when the clock A registers the time t, the clock B registers the time t' given by equation (11). Conversely, when the clock B registers the time t', the clock A should register the time t.

Instead, substituting equation (11) into equation (12) we do not obtain $t = t$ but:

$$t \neq t \left(1 - \frac{v^2}{c^2} \right)$$

This is a paradox or mathematically speaking an indeterminate form because we do not know which equation to use between (11) and (12) to determine t' or t given t or t' respectively.

5.2   A PTOLEMAIC WORLD

Science must agree with observations and so to find out which equation to use between (11) and (12) we consider a real case of the clock paradox and not the thought one known as the twin paradox.

We think of the muons coming from the upper parts of the Earth's atmosphere. These particles at rest decay in a lifetime $\tau_0 = 2.15 \cdot 10^{-6}$ s into an electron (positron) and two neutrinos. When in motion the lifetime will change according to one of the two relativistic time transformations.

For example, muons of total energy equal to 1 GeV travel at v/c = 0.9944087 in the reference frame R. Then from the point of view of an observer on the Earth, it follows from equation (11) that their lifetime τ is:

$$\tau = \frac{\tau_0}{\sqrt{1 - \dfrac{v^2}{c^2}}} = \frac{2.15 \cdot 10^{-6}}{\sqrt{1 - 0.9944087^2}} = 2.04 \cdot 10^{-5} \text{ s}$$

So, the length travelled by the muons through the atmosphere is:

$$L = v\tau = c\,\frac{v}{c}\,\tau = 299792458 \times 0.9944087 \times 2.04 \cdot 10^{-5} = 6081 \text{ m}$$

This result agrees with the experience. In fact, the muons are observed to travel through the layers of the atmosphere for several kilometers before they decay.

Now, considering special relativity as a Copernican theory, also the conclusions from the point of view of an observer seeing the muons at rest (frame R') should agree with observations. In the Copernican world there is not any preferred observer. To verify this, we calculate the lifetime τ of the muons in R according to the observer in R'. Using equation (12) we have:

$$\tau = \tau_0 \sqrt{1 - \frac{v^2}{c^2}} = 2.15 \cdot 10^{-6}\sqrt{1 - 0.9944087^2} = 2.27 \cdot 10^{-7} \text{ s}$$

Substituting this value into the relation $L = v\,t$, the observer in R' will derive that from the surface of the Earth (frame R) muons are seen to travel through the atmosphere for a distance L = 68 m which is in sharp disagreement with our observations. Hence, we can conclude that equation (12) is unphysical not describing the reality correctly.

At this point, we deduce that the results of the observer R' are just mathematical artifacts. That is also suggested by considering the length contraction. More precisely, as illustrated in the internet adaption of the book *Why God doesn't exist* by Bill Gaede, from the muon perspective, frame R', the muon is at rest and the Earth's atmosphere is rushing past it at 99.99% the speed of light. This means that the atmosphere is length contracted by a factor of $1/\gamma = 1/71$ allowing the muon to remain in existence long enough to make the trip. To the muon, length contraction is not merely a visual effect because the muon is not seeing anything. Hence, the distance to be travelled by the muon from the upper atmosphere to the sea level is physically shorter than the same distance measured from the Earth's surface. Then, because of a muon coming from the Sun, our planet and star should get close resulting in a solar power reaching us amplified by a factor of $71^2 = 5041$.

Obviously, that is not the case since such kind of amplifications have never been observed until now.

In conclusion, we have found that only the predictions of the observer in R are correct as confirmed by using equation (11), while the predictions of the observer in R' do not agree with the experimental evidence as we have verified by using equation (12). In this case, following the most obvious explanation, we can say that there is a preferred observer. Since the geocentric observer is the preferred one, it follows that special relativity provides a reliable result if embedded in a Ptolemaic world.

Now most of the readers will shook their heads but let us pause for a moment to think about it. Obviously, I am not denying the Copernican system in astronomy, instead I am suggesting that the Copernican philosophical framework based on equivalent observers could not be suitable in any case. Only the experience should define the extent of a general concept.

Conversely, if we really live in a Copernican world, special relativity must be corrected to satisfy this requirement. And if this is not possible, it could happen that a new theory may be introduced to replace it. However, this new theory should contain the basic laws of the old one. For example, the mass-energy equivalence $E = mc^2$ must be a part of it since this law has been proved to be a law of nature. In fact, the laws of nature do not change if the related physical theory is changed.

6. CONCLUSIONS

The study of the expansion of the outburst occurred in the M87 jet during the time period between the years 2001 and 2003 revealed that special relativity provides unreliable results. Conversely, considering a superluminal expansion emitting light travelling faster than light the results seem to be more reasonable. However, this fact should not be regarded as a refusal of special relativity.

In this article we agree with the considerations in ref. [15] where it is argued that special relativity, as formulated by Einstein, is a philosophical rather than a scientific theory. In fact, as indicated there, the total acceptance and complete adoption of Einstein's views made the relativistic mechanics the Einstein's theory. Instead, unlike relativistic mechanics, quantum mechanics is presented and adopted in its bare formalism and the different interpretations of this latter one, see for example the Copenhagen school, are left to the taste of the single scientist. For the sake of equality and scientific impartiality special relativity must be treated like quantum mechanics and so the Einstein interpretation of its bare formalism should be accepted or not according to the different personal opinions. Unfortunately, this was not the case until now. Coordinated and well-organized efforts are often used to suppress any sort of opposition. And the result is that unverified deductions become scientific facts.

In conclusion, there are two views of special relativity in this day and age. The first one considers each prediction of the theory as a real description of the physical phenomena even when the experimental support is missing or questionable. In this article some cases have been discussed. The other view instead is based on the search of any flaw in the relativistic mechanics to dismiss the whole theory. In the author's opinion, such situation with opposed positions will forbid any development of the scientific knowledge because the object, in the broadest sense of the term, is no longer the center of the debate but the personal views of it become the issue.

7. References

[1]   Hannu Karttunen et al. (Eds.), *Fundamental astronomy*, 5th Edition, Springer-Verlag Berlin Heildelberg 2007.

[2]   Juan P. Madrid, *Hubble Space Telescope observations of an extraordinary flare in the M87 jet*, The Astronomical Journal, 137:3864-3868, 2009 April.

[3]   D. Mazin et al., *M87: the 2010 very high energy gamma-ray flare & 10 years of multi-wavelength observations*, 33rd International Cosmic Ray Conference, Rio de Janeiro 2013.

[4]   John R. Taylor, *An introduction to error analysis*, 2nd Edition, University Science Books, Sausalito CA 1997.

[5]   Christopher Z. Waters and Stephen E. Zepf, *Ultraviolet Hubble Space Telescope observations of the jet in M87*, The Astrophysical Journal, 624:656-660, 2005 May 10.

[6]   D. E. Harris and Henric Krawczynski, *X-ray emission from extragalactic jets*, Annual Review of Astronomy and Astrophysics, 44:463-506, 2006 September 22.

[7]   J.A. Biretta et al., *Hubble Space Telescope observations of superluminal motion in the M87 jet*, The Astrophysical Journal, 520:621-626, 1999 August 1.

[8]   J.A. Biretta et al., *Detection of proper motions in the M87 jet*, The Astrophysical Journal, 447:582-596, 1995 July 10.

[9]   C. C. Cheung et al., *Superluminal radio features in the M87 jet and the site of flaring TeV gamma-ray emission*, The Astrophysical Journal, 663:L65-L68, 2007 July 10.

[10] A. Unzicker, *The Higgs fake: how particle physicists fooled the Nobel committee*, CreateSpace Independent Publishing Platform, 2013 October 9.

[11] G. Capezzali, *Inverted dynamics*, Physics Essays, 29:27-48, 2016 March 16.

[12] M. Antonello et al., *Precision measurement of the neutrino velocity with the ICARUS detector in the CNGS beam*, arXiv:1208.2629v2 [hep-ex], 2012 September 26.

[13] P. Alvarez Sanchez et al., *Measurement of CNGS muon neutrino speed with Borexino*, arXiv:1207.6860v1 [hep-ex], 2012 July 30.

[14] T. Adam et al., *Measurement of the neutrino velocity with the OPERA detector in the CNGS beam using the 2012 dedicated data*, arXiv:1212.1276v2 [hep-ex], 2012 December 17.

[15] N. Yu. Agafonova et al., *Measurement of the velocity of neutrinos from the CNGS beam with the Large Volume Detector*, arXiv:1208.1392v2 [hep-ex], 2012 August 23.

[16] Taha Sochi, *Special relativity: scientific or philosophical theory?*, arXiv:1610.0564v1 [physics.gen-ph], 2016 October 14.